HHS Public Access

Author manuscript

Apoptosis. Author manuscript; available in PMC 2022 February 01.

Published in final edited form as:

Apoptosis. 2021 February ; 26(1-2): 132–145. doi:10.1007/s10495-020-01654-w.

Characteristics of intracellular propagation of mitochondrial BAX recruitment during apoptosis

Joshua A. Grosser[1,2], **Margaret E. Maes**[3], **Robert W. Nickells**[1,4]

[1]Department of Ophthalmology and Visual Sciences, University of Wisconsin-Madison, 1300 University Ave, Madison, WI 53706, USA

[2]Wake Forest University School of Medicine, Winston-Salem, NC, USA

[3]Institute of Science and Technology Austria, Klosterneuburg, Austria

[4]McPherson Eye Research Institute, University of Wisconsin-Madison, Madison, WI, USA

Abstract

Recent advancements in live cell imaging technologies have identified the phenomenon of intracellular propagation of late apoptotic events, such as cytochrome c release and caspase activation. The mechanism, prevalence, and speed of apoptosis propagation remain unclear. Additionally, no studies have demonstrated propagation of the pro-apoptotic protein, BAX. To evaluate the role of BAX in intracellular apoptotic propagation, we used high speed live-cell imaging to visualize fluorescently tagged-BAX recruitment to mitochondria in four immortalized cell lines. We show that propagation of mitochondrial BAX recruitment occurs in parallel to cytochrome c and SMAC/Diablo release and is affected by cellular morphology, such that cells with processes are more likely to exhibit propagation. The initiation of propagation events is most prevalent in the distal tips of processes, while the rate of propagation is influenced by the 2-dimensional width of the process. Propagation was rarely observed in the cell soma, which exhibited near synchronous recruitment of BAX. Propagation velocity is not affected by mitochondrial volume in segments of processes, but is negatively affected by mitochondrial density. There was no evidence of a propagating wave of increased levels of intracellular calcium ions. Alternatively, we did observe a uniform increase in superoxide build-up in cellular mitochondria, which was released as a propagating wave simultaneously with the propagating recruitment of BAX to the mitochondrial outer membrane.

Robert W. Nickells, nickells@wisc.edu.

Author contributions J.G. and M.M. collected data. J.G. analyzed data. J.G. and R.N. designed experiments, interpreted results, and wrote the manuscript. All authors approved of the final draft.

Conflict of interest The authors declare no conflict of interest in the execution of this work. No patients or animals were used in these studies.

Compliance with ethical standards

Code Availability Not Applicable.

Publisher's Note Springer Nature remains neutral with regard to jurisdictional claims in published maps and institutional affiliations.

Supplementary Information The online version contains supplementary material available at https://doi.org/10.1007/s10495-020-01654-w.

Keywords

Intrinsic apoptosis; Asynchronous propagation; BAX; Mitochondrial outer membrane permeabilization; Superoxide

Introduction

The central events of intrinsic apoptosis are mitochondrial outer membrane permeabilization (MOMP) and the release of mitochondrial intermembrane proteins, events which are orchestrated by pro-apoptotic BAX recruitment to the mitochondrial outer membrane (MOM). While many cell types exhibit near simultaneous activation of intrinsic apoptosis, high speed live-cell imaging has recently revealed “waves” of apoptotic events, such as mitochondrial depolarization and cytochrome c release, propagating within cells during apoptosis [1–8]. However, not all cells exhibit this behavior, and few studies have been published on the subject. It is therefore unclear whether intracellular propagation is a universal phenomenon of apoptosis or whether it is confined to certain experimental parameters.

Studies on apoptosis propagation hint that the phenomenon applies broadly across cell lines, but more needs to be done to verify this. Eight cell models have been reported to display propagation of at least one apoptotic event to date (Table 1). A variety of death stimuli have been tested, indicating that the apoptotic stimulus is likely not responsible for the phenomenon. Because of the speed at which it occurs, observing apoptosis propagation is difficult, which may explain the relative lack of research. There is high variation, ranging from several hours to days, in when individual cells within a population undergo apoptosis following a death stimulus [5, 9, 10]. Despite the apoptotic window being hours to days long, MOMP and molecule release occur on the order of minutes, and apoptosis propagation likewise proceeds quickly, usually between 10 and 40 μm per minute within a given cell (Table 1). For example, HeLa cells are typically 17–30 μm in diameter, which gives the observer only a few minutes within the apoptotic window to record intracellular propagation [11]. Studies that report apoptosis propagation often catch it accidentally and then modify their methodology, such as fusing cells together to make the apoptotic field longer [3], to facilitate further investigation of this phenomenon.

The mechanism of apoptosis propagation is unknown. Most studies have investigated the role of calcium but results are often contradictory (Table 1). For example, Bhola and colleagues [4] successfully prevented cytochrome c release propagation by inhibiting HeLa cell sarco/endoplasmic reticulum Ca^{2+}-ATPase (SERCA) pumps with thapsigargin, while Lartigue et al. [3] found that thapsigargin had no effect on cytochrome c release propagation, also in HeLa cells. Investigators have manipulated reticulate calcium uptake, mitochondrial permeability transition pore (mPTP) release, and cytosolic calcium concentration with varying degrees of success (Table 1). Of note, none of these studies have used genetically encoded calcium indicators to track cellular calcium concentrations and instead have relied on recordings of calcium-sensitive dyes in permeabilized model systems.

Multiple pathways may contribute to apoptosis propagation, so some studies look for changes in propagation speed when probing whether a treatment has an effect. For example, Cheng and Ferrell [8] found that Ac-DEVD-CHO, a caspase inhibitor, significantly slowed the propagation velocity. Caspases cleave the BH3-only protein BID to an active form to promote mitochondrial involvement in apoptosis, and this positive feedback loop could facilitate apoptosis propagation [12, 12]. Three previous studies failed to prevent apoptosis propagation using zVAD-fmk, a different pan-caspase inhibitor. However, these groups did not measure propagation speed after caspase inhibition [2, 3, 6]. It should also be noted that apoptosis propagation speed varies significantly in the studies that report it, even within cell types. For example, Lartigue et al. [3] and Rehm et al. [5] both treated HeLa cells with 1 μM staurosporine (STS) and found that cytochrome c release propagated at 17.7 ± 3.3 and 10.2 ± 1.8 μm/min, respectively. Using differentiated and permeabilized H9c2 cells, Pacher and Hajnóczky [2] found mitochondrial depolarization to propagate at approximately 40 μm/min. With the same cell line, Garcia-Perez et al. [6] calculated a cytochrome c release propagation speed of 11.4 ± 0.6 μm/min. In Longtine et al. [7], apoptosis (as measured by mitochondrial depolarization and nuclear condensation) proceeded as slowly as 4.5 μm/min.

BCL-2 family modulation is another common intervention. Like caspase inhibition, Cheng and Ferrell [8] found that increasing BCL-2 concentration slows propagation speed. In Pacher and Hajnóczky [2], BCL-X overexpression reduced the percentage of cells exhibiting apoptosis propagation, and BID phosphorylase CK2 inhibition had the same effect [5]. Conversely, Lartigue and colleagues [3] detected no change in speed or occurrence of cytochrome c release propagation after BAX and BAK knockout. However, the syncytia used in this study were created by combining wildtype HeLa cells with B $ax^{-/-}$/$Bak^{-/-}$ mouse embryonic fibroblasts at a ratio of 1:2. BAX and BAK were therefore present in their model, albeit at lower concentrations. Despite the likely involvement of BCL-2 family proteins in propagating apoptosis across cells, propagation of BCL-2 family-events, such as BAX recruitment to the MOM, has not been published.

The present study is the first to report intracellular propagation of BAX recruitment, supporting the involvement of BAX as an upstream trigger of commonly reported propagating events such as cytochrome c release and caspase activation. We found that the speed of BAX recruitment propagation significantly correlated with cellular segment width, and we also observed that apoptosis can independently initiate at multiple points within a single cell. Contrary to a previous study [2], we found no evidence of a cytosolic calcium wave during apoptosis propagation. Finally, using MitoSOX, we found that mitochondrial superoxide slowly accumulates prior to BAX activation and is released during BAX recruitment, offering an additional positive feedback mechanism for the propagation of BAX activation.

Materials and methods

Tissue culture and nucleofection

ARPE-19 cells (immortalized human retinal pigmented epithelial cells) were cultured in DMEM:F-12 (Hyclone, GE Healthcare Life Sciences, Marlborough, MA) supplemented with 10% FBS (Atlanta Biologicals, Norcross, GA) and 1% penicillin streptomycin (Sigma,

St. Louis, MO) at 37 °C and 5% CO_2. For nucleofections (4D Nucleofector, Lonza, Basel, Switzerland), 3–5 μg of each plasmid DNA was used for reactions comprised of one million cells each. Nucleofected cells (350,000–500,000) were then plated on 35 mm glass bottomed (No. 1.5 optical grade) dishes (MatTek, Ashland, MA). Apoptosis was induced 24 h post-nucleofection using a final concentration of 1 μM STS (Sigma) prepared in DMSO. ARPE-19 cells were a gift from Dr. Aparna Lakkaraju (University of California-San Francisco, formerly University of Wisconsin-Madison) and were used in live-cell imaging experiments until passage 25. D407, 661 W, and HeLa cells were cultured and apoptosis induced as previously described [13]. Superoxide production was assessed in dying ARPE-19 cells by incubating them in 4 μM MitoSOX (Molecular Probes Inc., Eugene, OR) for 8 min prior to live cell imaging.

Plasmids

GFP-BAX, mCherry-BAX, and mito-BFP were cloned in the lab as previously described ([10, 14]). The vector backbone for these plasmids include peGFP-C3 and pmCherry-C1 (Clontech, Mountainview, CA) and TagBFP-N (Evrogen, Moscow, Russia). All transgenes were expressed from the CMV immediate early promoter. Cytochrome c-GFP (Addgene, Cambridge, MA, plasmid #41,182) and SMAC-GFP (Addgene plasmid #40,881) were gifts from Douglas Green [15]. The calcium reporter plasmid pN1-GCaMP6m-XC (Addgene, plasmid #111,543) was a gift from Xiaodong Liu [16]. Reporter function of this plasmid was verified in ARPE-19 cells using the divalent cation ionophore A23187 at a final concentration of 10 μM (Abcam, Cambridge, UK).

Image acquisition

Culture media was replaced with recording media (1.26 μM $CaCl_2$, 0.49 μM $MgCl_2 \cdot 6H20$, 0.41 μM $MgSO_4 \cdot 7H20$, 5.33 μM KCl, 0.44 μM H_2PO_4, 4.2 μM $NaHCO_3$, 13.8 μM NaCl, 0.34 μM H PO_4, 5 g/L glucose, and 10 μM Hepes) prior to imaging. For MitoSOX experiments, MitoSOX (Thermo Fisher Scientific, Waltham, MA) was added to the recording media (final concentration 4 μM) and the cells were incubated for 8 min. The MitoSOX media was then replaced with regular imaging media. Live-cell imaging was performed using the Andor Revolution XD spinning disk confocal microscopy system (Andor, Belfast, Northern Ireland) comprised of the Nikon Eclipse Ti inverted microscope, Nikon objectives, the iXon × 3 897 EM-CCD camera, a Yokogawa CSU-X1 confocal spinning disk head, the Andor Laser Combiner with four solid state lasers, an ASI motorized stage with Piezo-Z, and an Okolab CO_2 cage incubator for temperature and CO_2 control at 37 °C and 5% CO_2 (CO_2 was kept off during the experiments). Using the time-lapse function, ARPE-19 images were taken every 10 min, 2 min, or 5 s beginning 14–17 h post STS addition. 661 W, D407, and HeLa cells were imaged as previously described [13]. All images were taken at 100X (oil, numerical aperture = 1.49, temperature collar for 23–37 °C) and consisted of 20–30 optical sections of 0.22 μm (Nyquist). All imaging was performed under the same laser intensity, electron-multiplying gain, and exposure time.

Image analysis

All analysis was performed using IMARIS 9.2.1. Two separate methods were utilized to measure BAX propagation. In the first “end-to-end” method, the ‘Spots’ function was used

to manually sample fluorescent intensities regions of interest (ROIs) every 10 μm from one end of the cell to the other. BAX recruitment, SMAC release, and cytochrome c release were defined as 125% baseline fluorescence, 75% baseline fluorescence, and 75% baseline fluorescence, respectively. The second, "refined" method measured propagation velocity over small lengths of cell processes. Here, the distance of propagation, which was determined by measuring the progress of the recruitment/release wave-front over 1–2 frames, was divided by the time between frames to determine velocity. The average width of the segment of process was also recorded. When comparing these velocities to mitochondrial volume, the 'Surfaces' function was used to model Mito-BFP fluorescence in the length of cell that propagation speed was measured. When comparing these velocities to the mitochondrial to cytosol ratio, the 'Surfaces' function was also used to model diffuse mCherry-BAX fluorescence one frame before recruitment (at which time diffuse mCherry-BAX functioned as a cell-fill). All images within a single figure were prepared using the same brightness, contrast and color adjustments in Photoshop.

Statistical analysis

For comparing the proportions of cells exhibiting apoptosis propagation, we used a chi-square test. With sample sizes under 10, a Fisher's exact test was used instead of the chi square test. Spearman correlations were used to compare relationships between propagation speed and process width, mitochondrial volume, and mitochondrial density. For comparing average mitochondrial densities, a two-tailed, unpaired t-test assuming unequal variance was used. Significance was set to $\alpha = 0.05$ for statistical tests. All averages are presented as mean ± 95% confidence interval.

Results

BAX recruitment propagates in subsets of 661 W, HeLa, D407, and ARPE-19 cells

BAX recruitment propagates intracellularly in subsets of cells in four different cell lines. Of the cells that underwent apoptosis, BAX recruitment propagation was observable in 43.5% of 661 W cells (n = 23) (Fig. 1a–d), 12.9% of HeLa cells (n = 62) (Fig. 1e–h), and 14.8% of D407 cells (n = 108) (Fig. 1i–l) when imaging every minute. The remaining sections focus on the ARPE-19 cell line, which were induced for apoptosis with 1 μM STS 24 h after being nucleofected with mCherry-BAX, Mito-BFP, and either SMAC-GFP or Cytochrome c-GFP. Intracellular propagation of BAX recruitment was observed in 68 of the 114 ARPE-19 cells captured undergoing apoptosis (~ 60%).

BAX recruitment, cytochrome c release, and SMAC release propagate together

In propagating ARPE-19 cells co-expressing cytochrome c-GFP or SMAC-GFP with mCherry-BAX, the point(s) of initiation and direction of release propagation aligned with the initiation point(s) and direction of BAX recruitment propagation in every cell (n = 21) (Fig. 2a, Supplemental Videos 1 and 2). For each cell, the times of recruitment/release relative to the initiation time were measured at ROIs set in increments of 10 μm, starting at the initiation location. The times of recruitment/release at each 10 μm ROI were then plotted (mean ± SE) against the distance from the initiation location (Fig. 2b). The linear relationship between variables was significant for each protein (BAX: $r^2 = 0.984$, $p <$

0.00001; SMAC: $r^2 = 0.883$, $p < 0.05$; cytochrome c: $r^2 = 0.944$, $p < 0.05$). At each 10 μm increment, no statistical difference existed between the times of BAX recruitment, cytochrome c release, or SMAC release (Fig. 2b).

Formation of processes increases the likelihood of BAX recruitment propagation

The larger proportions of ARPE-19 and 661 W cells exhibiting BAX recruitment propagation is possibly attributable to an effect of STS on the morphology of these cell lines. STS addition to ARPE-19 cells typically resulted in the peripheral soma retracting over several hours, leaving behind a smaller soma with multiple thin processes (Fig. 3a–j, Supplemental Video 3). 661 W cells, another immortalized oular-derived cell line, exhibit a similar morphological response to a sub-lethal dose of STS after 24 h [17]. The change in morphology is note-worthy because ARPE-19 cells with processes were significantly more likely to exhibit propagation of BAX recruitment [χ^2 ($N = 114$) = 31.25, $p < 0.00001$]. The likelihood of propagation also correlated with cell length (reflecting longer processes) (Fig. 3k). Cells with a maximum length of 30–60 μm were significantly more likely to exhibit propagation over cells < 30 μm [χ^2 ($N = 65$) = 4.95, $p = 0.026$], while cells reaching 60–90 μm in length were more likely to propagate relative to cells 30–60 μm [χ^2 ($N = 80$) = 10.44, $p = 0.001$]. Cells extending longer than 90 μm were not significantly more likely to propagate than cells between 60 and 90 μm [χ^2 ($N = 50$) = 0.42, $p = 0.516$].

It was also common to observe asynchronous propagation only within a cell's processes, while recruitment appeared synchronous in the majority of the cell somas. To evaluate if somal propagation was occurring too rapidly to be captured at our normal imaging speed of 1 image every 10–2 min, we increased imaging speed to one image every 5 s. This, however, did not increase the likelihood of observing BAX recruitment propagation in the soma, nor did it significantly increase the likelihood of observing apoptosis propagation in cells without processes (Fig. 3l).

Cellular processes often act as initiation sites for BAX recruitment

BAX recruitment was more likely to initiate in a cellular process. Of the 68 ARPE-19 cells which clearly displayed BAX recruitment propagation, recruitment began in one or more processes in 61 cells (~ 90%), suggesting that environmental and/or cellular conditions in the process make that area more conducive to the initiation events leading to BAX recruitment and apoptosis. In 42 of these cells, BAX recruitment began at a single point, usually the distal end of a process, and proceeded directionally throughout the remainder of the cell (Fig. 4a–d). In cells exhibiting this behavior, propagation was often observed to be synchronous in the soma and then continued asynchronously in other processes, starting from the proximal end of the process and extending distally. In 15 cells, BAX recruitment initiated in two processes separately and traveled to the remainder of the cell (Fig. 4e–h). In 4 cells exhibiting BAX recruitment propagation, three-point initiation was observed (Fig. 4i–l). In cells with multiple point initiation, the second and third points of initiation typically occurred after the initial point of BAX recruitment. The final pattern of BAX recruitment was synchronous recruitment, which was seen in ~ 40% of cells undergoing apoptosis (Fig. 4m–p).

The average end-to-end speed of BAX recruitment propagation was 6.99 ± 1.95 μm/min. This measurement is both slower and more variable than others reported in the literature (Table 1). The existence of thin, STS-induced processes (see Sect. Formation of processes increases the likelihood of BAX recruitment propagation) probably accounts for this discrepancy. Specifically, we observed that BAX recruitment propagation traveled significantly slower in thinner cellular segments (rank Spearman correlation, rs[36] = 0.784, $p < 0.001$) (Fig. 5).

Analysis of factors that may account for BAX recruitment propagation in processes

Previous reports in the literature have suggested several factors that may co-ordinate the propagation of mitochondrial apoptotic events. Cheng and Ferrell [8] found that increasing the concentration of mitochondria in in vitro cytosol assays resulted in higher propagation speeds, so we hypothesized that either the mitochondrial volume (V_m) or density (V_m to $V_{cytosol}$) within cellular segments would positively correlate with propagation speed in those segments. Mitochondrial volume was measured with Imaris in Z-stacks using Mito-BFP, and cytosol volume was measured using diffuse mCherry-BAX one frame before BAX recruitment began. Mitochondrial volume did not correlate with propagation speed (rank Spearman correlation, rs[23] = 0.275, $p = 0.203$). Surprisingly, a negative correlation was measured between mitochondrial density and propagation speed (rs[21] = −0.493, $p < 0.05$). Similarly, mitochondrial concentrations do not account for the difference in synchronous propagation in processes and asynchronous propagation in somas. We found that the average densities of mitochondria in processes and somas were not significantly different (0.11 $\mu m^3_m/\mu m^3_{cytosol}$ in the processes versus 0.086 $\mu m^3_m/\ \mu m^3_{cytosol}$ in the somas, $p = 0.22$).

To investigate calcium's role in the propagation of apoptotic events, we used the fluorescent intracellular free calcium indicator pN1-GCaMP6m-XC to visualize cytosolic calcium concentrations before, during, and after apoptosis. There were no changes in cytosolic calcium detected before or during BAX recruitment (n = 10) (Fig. 6, Supplemental Video 4). All cells experienced a final burst of intracellular calcium 37.5 ± 8.2 min following BAX recruitment. At higher temporal resolutions (1 image every 2 min or faster), this calcium burst could be seen as a continuous, propagating wave, taking 8 ± 2.26 min (n = 4) to complete. Multiple discrete calcium spikes were also observed after BAX recruitment in all cells imaged at this temporal resolution (Fig. 6). These calcium events occurred in both synchronous and propagating cells.

We next used MitoSOX, a mitochondrial superoxide indicator, to test whether mitochondrial superoxide generation preceded the BAX recruitment wave, such that superoxide in neighboring mitochondria trigger the dysfunction of subsequent mitochondria. MitoSOX fluorescence increased in all mitochondria prior to BAX recruitment in all cells examined (n = 12) (Fig. 7a–h). In propagating cells, there was no clear correlation between the spatiotemporal pattern of mitochondrial superoxide accumulation and BAX recruitment propagation. However, mitochondrial MitoSOX fluorescence decreased rapidly part way through BAX recruitment, possibly as a result of MOMP (Fig. 7i–l, Supplemental Fig. S1). This observation suggests a hypothesis that the release of superoxide into the cytosol acts as an initiator of further BAX recruitment during propagation.

Discussion

BAX recruitment propagated in subsets of ARPE-19, 661 W, D407, and HeLa cells, although the proportion of these cells exhibiting recruitment propagation varied. When co-nucleofected with cytochrome c-GFP or SMAC/Diablo-GFP, the spatiotemporal pattern of BAX recruitment and mitochondrial protein release aligned in every cell. The morphological change induced by STS in the ARPE-19 and 661 W cell lines likely accounted for the large proportion of cells where BAX recruitment propagation was appreciable compared to other cell types. Processes lengthen the distance that BAX recruitment and mitochondrial intermembrane molecule release can propagate, making observing these events more likely. Recruitment also propagated slower in thinner cellular segments and was more likely to initiate focally in the extreme tips of processes.

While single-point initiation was most common, two-point initiation was observed frequently, and three-point initiation was observed in a small number of cells. Local BAX recruitment initiation places susceptibility to BAX activation on the subcellular level, at least some of the time. One possibility is that the least healthy or most metabolically active mitochondrion serves as the “weakest link,” whose failure spreads to the rest of the mitochondrial chain. In support of this possibility, Garcia-Perez et al. [6] found that the superoxide dismutase (SOD2) mimetic MnTMPyP, a reactive oxygen species (ROS) scavenger, reduced the speed of propagation, as did mitochondrial SOD2 overexpression. Using MitoSOX, the authors found that the spatiotemporal pattern of superoxide generation in the mitochondrial matrix correlated with the propagating release of cytochrome c. We performed this experiment in our own study but were unable to validate these findings. We did, however, find that MitoSOX fluorescence in the mitochondria increased prior to BAX recruitment and then decreased rapidly during BAX recruitment, the latter likely being a consequence of MOMP. The dispersion of superoxide after BAX recruitment may be capable of propagating the death signal intracellularly by creating successive microenvironments that enhance BH3-only protein activity [6]. Future studies might test whether a cytosolic wave of ROS accumulation exists during apoptosis, or whether BAX recruitment is more likely to initiate at highly active mitochondria.

A central question raised by this study is why 40% of ARPE-19 cells, many somas of propagating cells, and the majority of D407, 661 W, and HeLa cells displayed synchronous recruitment of BAX during apoptosis. Synchronous execution of occasionally propagating events in portions of cells has been reported in four of the seven live-cell imaging studies, but the simultaneous display of synchronous and propagating apoptosis within individual cells, as is the case when the process propagates and the soma does not, has not been mentioned. One possibility, which was first postulated by Bhola and colleagues [4], is that multi-point initiation is mistaken for synchronous apoptosis. It may even be impossible to distinguish between these two phenomena. This hypothesis explains simultaneous recruitment in fully-synchronous cells, but it does not explain the commonly observed behavior involving BAX recruitment propagating down a process before being recruited synchronously in the soma. We tested whether differences in mitochondrial density might explain this behavior because mitochondrial density has been shown to influence propagation speed, both in this study and another (although to opposite effects) [8].

However, no significant difference between the mitochondrial densities of processes and somas was found.

Another possibility is that, because there is variance in how fast recruitment propagates, rapidly propagating outliers may appear synchronous. The relationship established between cellular width and propagation speed supports this as an explanation for why processes usually propagate and somas usually do not. Increasing the imaging speed from 1 image every 10 min to 1 image every 2 min increased the proportion of cells exhibiting somal propagation in our study. Further increasing the imaging speed to 1 image every 5 s, however, did not reveal further evidence of somal propagation. The average somal diameter of 30 randomly sampled cells in this study was 14.3 ± 1.5 μm. Using the width vs propagation speed graph in Fig. 5, and assuming a linear relationship, the speed of propagation in the soma would be approximately 60 μm/min. Traveling across a 14.3 μm soma would take 14.3 s at this speed and would have been observable at the highest temporal resolution (1 image every 5 s). A non-linear relationship between width and speed might explain this discrepancy, as could limitations in our ability to detect 60 μm/min propagation speeds over short distances. BAX recruitment to individual mitochondria occurs more gradually than mitochondrial protein release [10]. This makes rapidly propagating BAX recruitment more difficult to measure because the gradient of fluorescent intensities produced by propagation is less appreciable over a given distance (to further illustrate, the contrast between punctate and diffuse SMAC over the same distance would be greater, since SMAC is released faster).

The last possibility is that, because molecular pathways leading to BAX activation are redundant, factors upstream of BAX may determine whether its recruitment to the MOM propagates. Modification of latent BH3-only proteins might account for the initiation of propagation in processes, allowing for transcriptionally regulated BH3 proteins to proceed and be present in the soma. PUMA, for example, is regulated primarily at the transcriptional level, whereas BIM and BAD reside in the cytosol and are regulated post-translationally [18]. It might also be that synchronous or rapidly propagating recruitment is initiated by more potent BH3 proteins such as PUMA, whereas slower, observable recruitment propagation is propelled by less effective BH3 proteins, such as NOXA [18]. Changing proportions of BH3 involvement may also help explain the wide range of propagation speeds reported in the literature. Future studies may investigate whether propagation speeds differ when apoptosis is induced using different BH3-only proteins.

We found no evidence that apoptosis propagation was prompted by a calcium wave, as has been reported [2]. We did, however, observe multiple calcium spikes and a full-cell calcium wave approximately forty minutes after BAX recruitment. Multiple studies have investigated calcium’s role in facilitating apoptosis propagation, but findings are contradictory. Bhola et al. [4] and Lartigue et al. [3] both measured cytochrome c release propagation in HeLa cells induced to die via STS. As was mentioned earlier, thapsigargin (a SERCA pump inhibitor) successfully prevented apoptosis propagation in the former but not the latter. Bhola and colleagues also tried buffering cytosolic calcium. Apoptosis propagation continued as normal, so the authors concluded that calcium signaling is primarily transmitted through mitochondria-associated membranes, which are close contacts (“quasi-synapses”) between

endoplasmic reticula and mitochondria ([19], reviewed in [20, 20]). It is unlikely that the GCaMP indicator used in this study would have detected microdomain calcium changes, such as those transmitted through these contacts. In congruence with our conclusions, the Lartigue study did not see any effect on cytochrome c release propagation after buffering cytosol calcium and emptying intracellular calcium stores.

Two studies from the same laboratory [2, 6] have examined calcium's role in apoptosis propagation using a cardiac myotube model (permeabilized and differentiated H9c2 cells). The first study [2] described two sequential calcium waves: first a rapid, low amplitude wave, closely followed by a slower, larger amplitude wave. Detecting the first calcium wave, which the authors reported travelled at 20 μm/s, would have been unlikely at our temporal resolution. The second wave, however, likely would have been observed had it occurred because it traveled at the same speed as mitochondrial depolarization, which has been shown to occur at approximately the same time as cytochrome c release [4, 8, 15]. This element of apoptosis propagation may therefore depend on the apoptotic stimulus or cell line. Calcium chelation using EGTA successfully halted apoptosis propagation in the first study, as did Ruthenium Red (RuRed), a ryanodine inhibitor, and cyclosporin A (CSA), a mPTP inhibitor. The second study, however, found no effect of CSA, RuRed, or EGTA [6]. The main difference is that these cells were induced to die with truncated BID (a BH3-only protein), whereas in the first study, apoptosis propagation was initiated with caffeine or calcium after treatment with an apoptotic stimulus (either ethanol or C2 ceramide). One possible explanation is that, while calcium can propagate the apoptotic signal by itself at high concentrations (such as those induced with caffeine or calcium itself in cardiac cells), spontaneous apoptosis involves a more diverse set of propagating death signals. Another possibility is that the calcium waves induced by adding caffeine or calcium to cardiac myotubes do not normally occur during apoptosis. The lack of cytosolic calcium waves during apoptosis in this present study supports these possibilities.

In conclusion, multiple studies have recently described the propagation of apoptotic events such as caspase activation and cytochrome c release. Although BAX has been proposed as a potential upstream trigger, the intracellular propagation of BAX recruitment has not been demonstrated until now. The documentation of apoptosis propagation is part of the broader necessity to elucidate the kinetics and mechanisms of apoptosis.

Supplementary Material

Refer to Web version on PubMed Central for supplementary material.

Acknowledgements

This work was supported by National Institute of Health grants R01 EY030123, P30 EY016665, and T32 GM081061, an unrestricted research grant from Research to Prevent Blindness, Inc., and the Frederick A. Davis Endowment from the Department of Ophthalmology and Visual Sciences at the University of Wisconsin-Madison.

Data availability

The datasets generated and analyzed for the current study are available from the corresponding author on reasonable request.

References

1. Cowan CM, Thai J, Krajewski S, Reed JC, Nicholson DW, Kaufmann SH, Roskams AJ (2001) Caspases 3 and 9 send a pro-apoptotic signal from synapse to cell body in olfactory neurons. J Neurosci 21:7099–7109 [PubMed: 11549720]
2. Pacher P, Hajnóczky G (2001) Propagation of the mitochondrial signal by mitochondrial waves. EMBO J 20:4107–4121 [PubMed: 11483514]
3. Lartigue L, Medina C, Schembri L et al. (2008) An intracellular wave of cytochrome c propagates and precedes Bax redistribution during apoptosis. J Cell Sci 121:3515–3523 [PubMed: 18840646]
4. Bhola PD, Mattheyses AL, Simon SM (2009) Spatial and temporal dynamics of mitochondrial membrane permeability waves during apoptosis. Biophys J 97:2222–2231 [PubMed: 19843454]
5. Rehm M, Huber HJ, Hellwig CT, Anguissola S, Dussmann H, Prehn JHM (2009) Dynamics of outer mitochondrial membrane permeabilization during apoptosis. Cell Death Differ 16:613–623 [PubMed: 19136937]
6. Garcia-Perez C, Roy SS, Naghdi S, Lin X, Davies E, Hajnóczky G (2012) Bid-induced mitochondrial membrane permeabilization waves propagated by local reative oxygen species (ROS) signaling. Proc Natl Acad Sci USA 109:4497–4502 [PubMed: 22393005]
7. Longtine MS, Barton A, Chen B, Nelson DM (2012) Live-cell imaging shows apoptosis initiates locally and propagates as a wave throughout syncytiotrophoblasts in pimary cultures of human placental villous trophoblasts. Placenta 33:971–976 [PubMed: 23102999]
8. Cheng X, Ferrell JE Jr (2018) Apoptosis propagates through the cytoplasm as trigger waves. Science 361:607–612 [PubMed: 30093599]
9. Prise KM, Folkard M, Michael BD (2003) A review of the bystander effect and its implications for low-dose exposure. Rad Protect Dos 104:347–355
10. Maes ME, Schlamp CL, Nickells RW (2017) Live-cell imaging to measure BAX recruitment kinetics to mitochondria during apoptosis. PLoS ONE 12:e0184434 [PubMed: 28880942]
11. Nath B, Raza A, Sethi V, Dalal A, Ghosh SS, Biswas G (2018) Understanding flow dynamics, viability and metastatic potencu of cervical cancer (HeLa) cells through constricted microchannel. Sci Reports 8:17357
12. Li H, Zhu H, Yuan J (1998) Cleavage of BID by caspase 8 mediates the mitochondrial damage in the Fas pathway of apoptosis. Cell 94: 491–501; Slee EA, Keogh SA, Martin SJ (2000) Cleavage of BID during cytotoxic drug and UV radiation-induced apoptosis occurs downstream of the point of Bcl-2 action and is catalysed by caspase-3: a potential feedback loop for amplification of apoptosis-associated mitochondrial cytochrome c release. Cell Death Differ 7:556–565 [PubMed: 9727492]
13. Maes ME, Grosser JA, Fehrman RL, Schlamp CL, Nickells RW (2019) Completion of BAX recruitment correlates with mitochondrial fission during apoptosis. Sci Reports 9:16565
14. Semaan SJ, Nickells RW (2010) The apoptotic response in HCT116$^{BAX-/-}$ cancer cells becomes rapidly saturated with increasing expression of a GFP-BAX fusion protein. BMC Cancer 10:554 [PubMed: 20942963]
15. Goldstein JC, Waterhouse NJ, Juin P, Evan GI, Green DR (2000) The coordinate release of cytochrome c during apoptosis is rapid, complete, and kinetically invariant. Nat Cell Biol 2:156–162 [PubMed: 10707086]
16. Yang Y, Liu N, He Y et al. (2018) Improved calcium sensor GCaMP-X overcomes the caclium channel perturbations induced by the calmodulin in GCaMP. Nat Commun 9:1504 [PubMed: 29666364]
17. Thompson AF, Crowe ME, Lieven CJ, Levin LA (2015) Induction of neuronal morphology in the 661W cone photoreceptor cell line with staurosporine. PLoS ONE 10:e0145270 [PubMed: 26684837]
18. Adams JM, Cory S (2007) The Bcl-2 apoptotic switch in cancer development and therapy. Oncogene 26:1324–1337 [PubMed: 17322918]
19. Csordás G, Thomas AP, Hajnóczky G (1999) Quasi-synaptic calcium signal transmission between endoplasmic reticulum and mitochondria. EMBO J 18:96–108 [PubMed: 9878054]

20. Grimm S (2012) The ER-mitochondria interface: the social network of cell death. Biochim. Biophys. Acta 1823: 327–334; Giorgi C, Missiroli S, Patergnani S, Duszynski J, Wieckowski MR, Pinton P (2015) Mitochondria-associated membranes: composition, molecular mechanisms, and physiopathological implications. Antioxid Redox Signal 22:995–1019 [PubMed: 22182703]

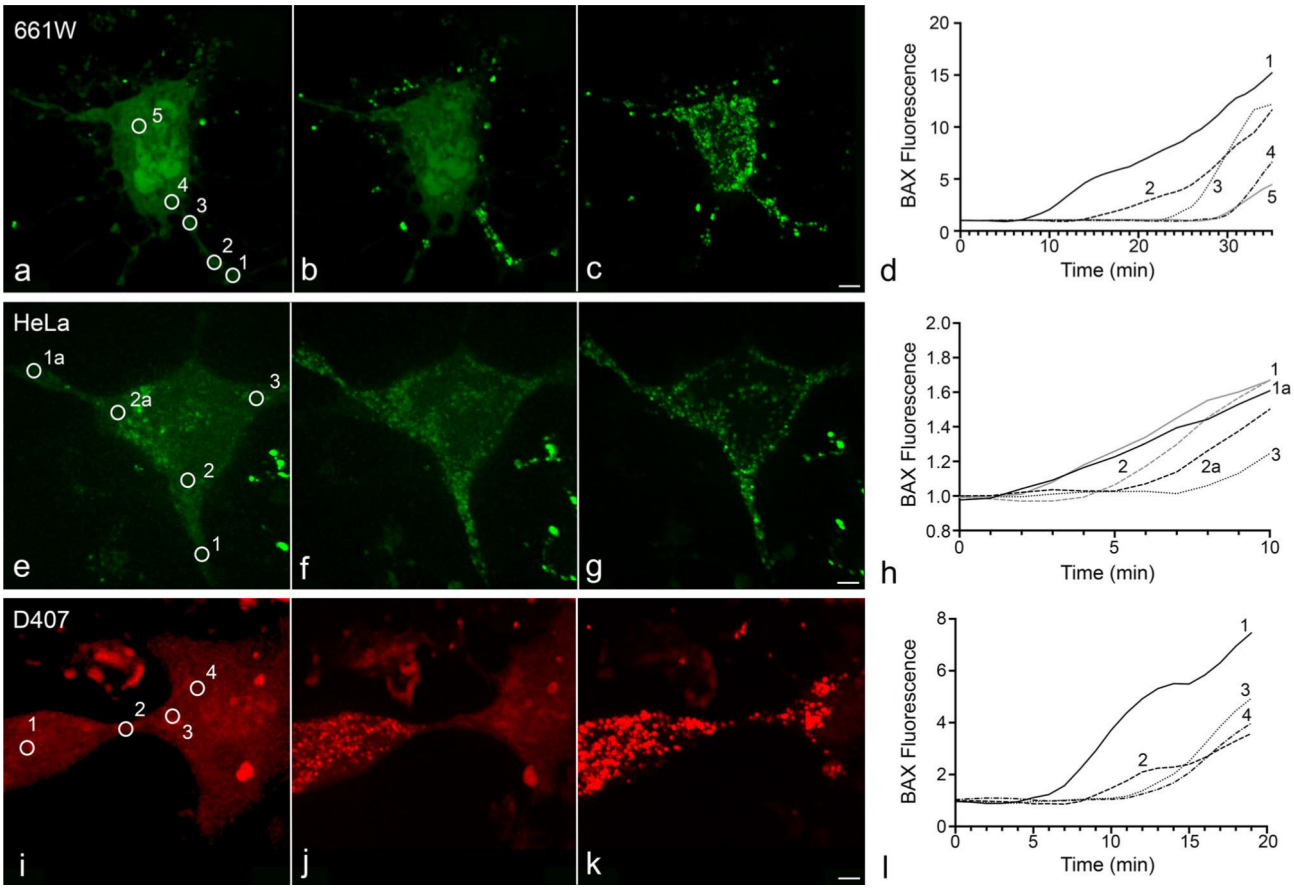

Fig. 1.

Propagation of BAX recruitment to the mitochondrial outer membrane in D407, 661 W, and HeLa Cells. The cells shown were nucleofected with either mCherry-BAX or GFP-BAX. D407 and HeLa cells were induced to die using 1 μM STS. Apoptosis in 661Ws was stimulated by overexpression of HDAC3 after differentiation using a sublethal dose (316 nM) of staurosporine. Examples of BAX recruitment propagation in 661 W (**a–d**), HeLa (**e–h**), and D407 (**i–l**) cells are included alongside graphs showing the staggered initiation of BAX recruitment (normalized to baseline fluorescence) at different numbered regions of interest (circled in micrographs **a**, **e**, and **i**). Size bars = 5 μm

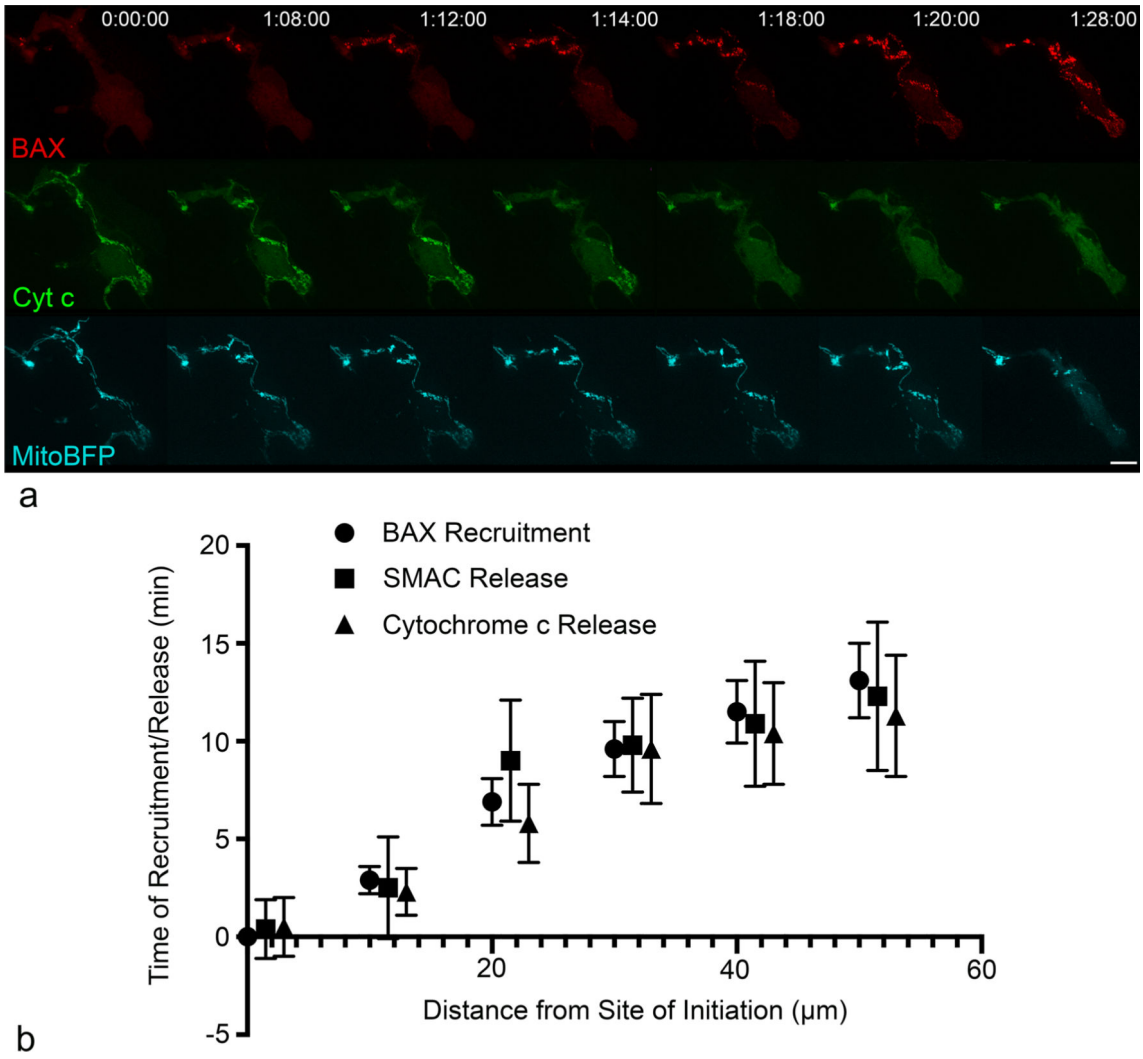

Fig. 2.

BAX recruitment, cytochrome c release, and SMAC release propagate together in ARPE-19 cells. The stills shown are of a cell nucleofected with mCherry-BAX, Cytochrome c-GFP, and Mito-BFP. BAX recruitment and cytochrome c release was initiated approximately 19 h post-STS in the cell shown. The time stamp at the top-left corner of the images for mCherry-BAX indicate the time relative to the start of the imaging session. BAX recruitment and cytochrome c release began at the 1 hr 8 min time stamp and propagated to the soma over the course of approximately 10 min (**a**) (See Supplemental Video 1 for example of Cytochrome c-GFP release and Supplemental Video 2 for SMAC-GFP release). Size bar = 10 μm. The average time (mean ± SE) of BAX recruitment (n = 47), cytochrome c release (n = 10), and SMAC release (n = 14) relative to the earliest time and location of BAX recruitment are plotted (**b**). The relationships between variables was significantly linear for each molecule (BAX: $r^2 = 0.984$, $p < 0.00001$; SMAC: $r^2 = 0.883$, $p < 0.05$; cytochrome c: $r^2 = 0.944$, $p < 0.05$). At each distance, there was no statistical difference between the times of BAX recruitment, cytochrome c release, or SMAC release

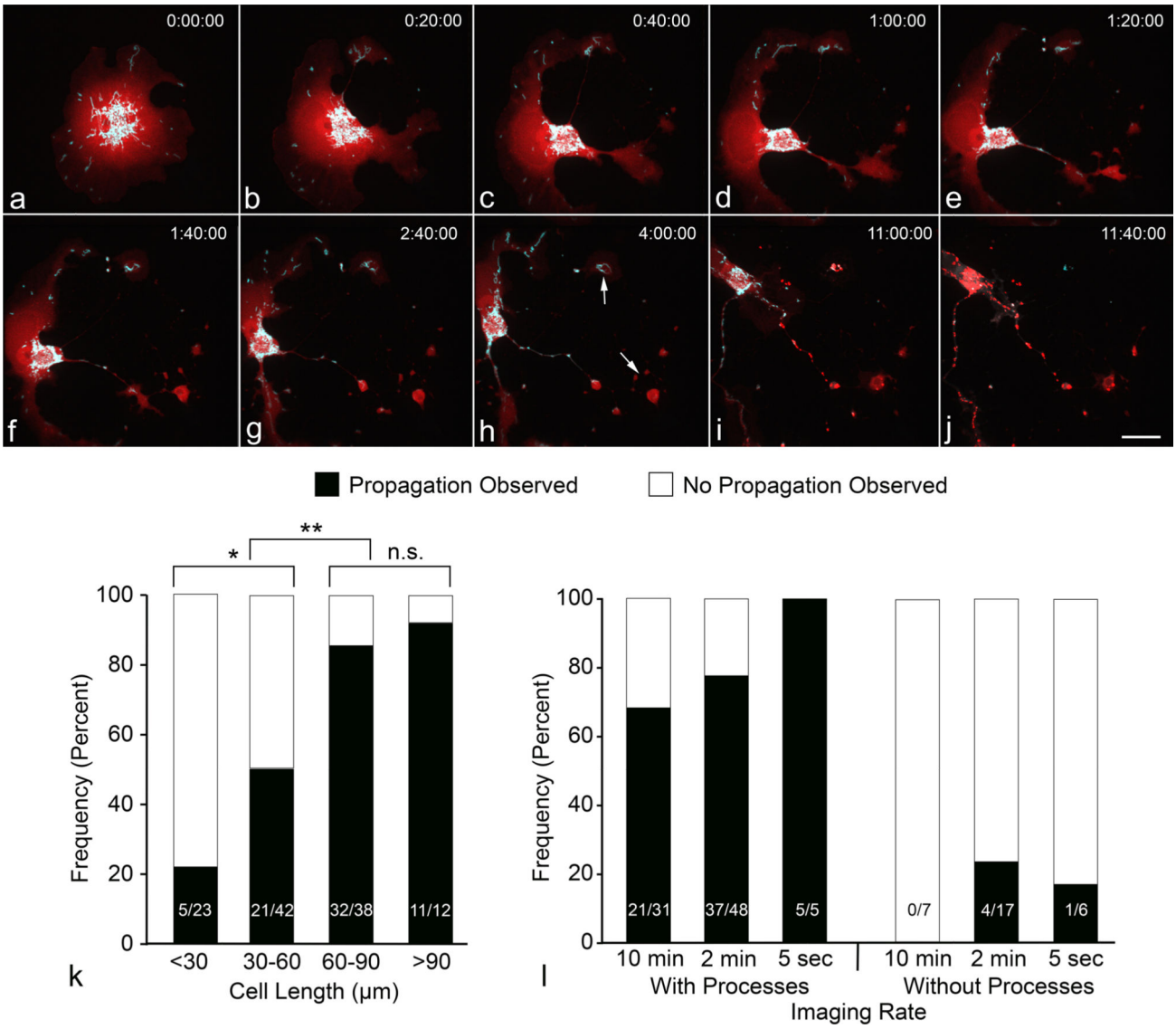

Fig. 3.

Presence of cellular processes increases the chance of observing BAX recruitment propagation. The ARPE-19 cell in this figure was nucleofected with mCherry-BAX and Mito-BFP. STS (1 μM) was added after 24 h of incubation, and imaging began immediately thereafter as to capture the STS-induced change in morphology (**a–h**). Size bar = 10 μm. BAX recruitment later initiated in the rightmost processes (arrows in panel h) and propagated to the soma (**i, j**). The maximum length of a cell (cell length as a surrogate for longer processes) correlated with an increased likelihood to show propagation of BAX recruitment (**k**) (*p = 0.026, **p = 0.001). The increase in BAX propagation frequency from 60–90 μm to > 90 μm was not statistically significant (n.s.). Increasing the imaging speed from 1 image every 10 min to 1 image every 2 min allowed for the occasional observation of BAX recruitment propagation in cells without processes (**l**), but overall the proportion of propagating cells was not significantly increased with faster imaging rates in either group of cells

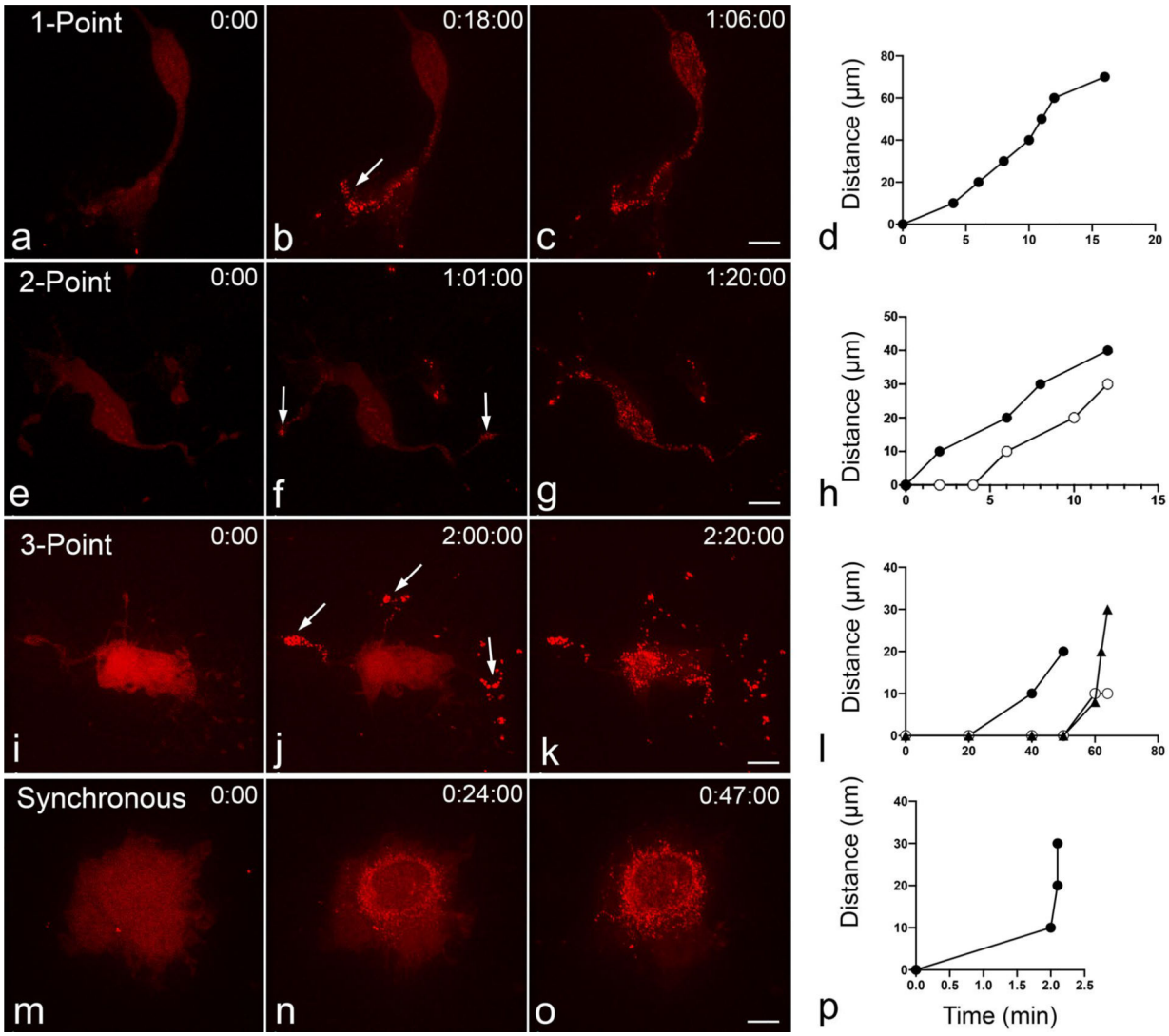

Fig. 4.

Cells with multi-point, and synchronous initiation of BAX recruitment. The cells shown were nucleofected with mCherry-BAX and induced to die using 1 µM STS. BAX recruitment was observed to independently initiate in 1 (**a–d**), 2 (**e–h**), or 3 (**i–l**) locations (indicated by arrows). Many cells (~ 40%) displayed synchronous recruitment of BAX as well (**m–p**). Size bars = 10 µm. Each graph shows a plot of BAX recruitment for each cell depicted. For the cells with 2 or 3 independent initiation points, the time that BAX is recruited in additional processes is shown relative to the time of the first site of initiation and the distance from that point. These cells show that multiple initiation points do not occur simultaneously in cells that exhibit them

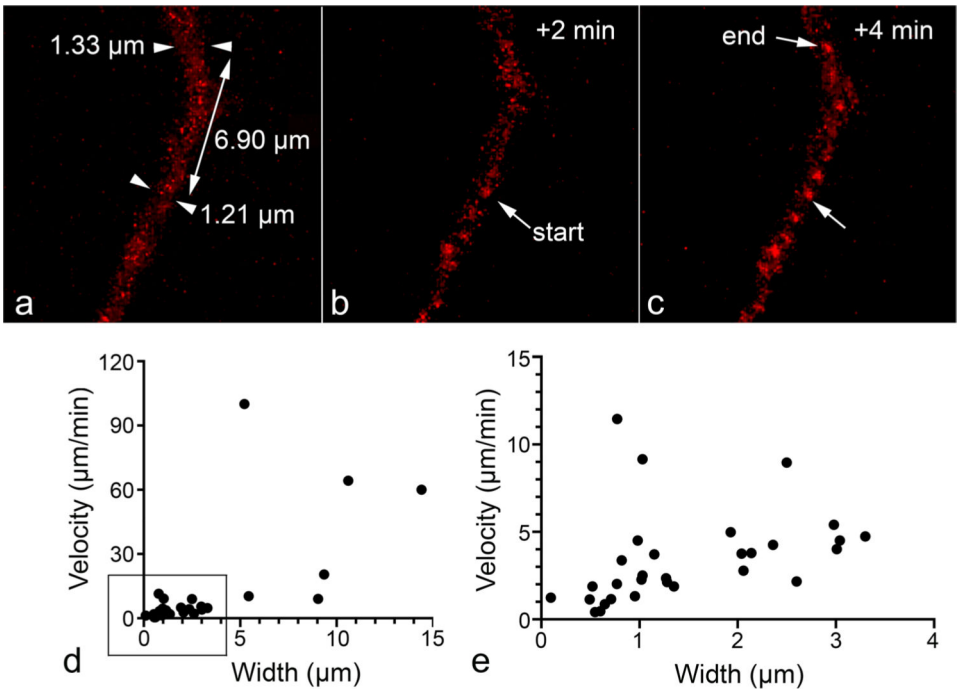

Fig. 5.

Velocity of BAX recruitment propagation correlates with width of process segment. The cell shown was nucleofected with mCherry-BAX and induced to die using 1 μM STS. The stills demonstrate the "refined" method of measuring propagation speed, described in Sect. Image Analysis of the methods. Using cellular processes with consistent widths, we measured how far the BAX recruitment wave-front traveled in 1 frame and divided this distance by the time between frames. **a–c** Example of a cellular process over 3 time frames of imaging showing the frame before initiation (**a**, arrowheads indicate process width measurements), at initiation ("start" arrow in **b**), and after movement of the propagating wave ("end" arrow in **c**). The velocity of BAX recruitment propagation was then plotted against the cellular segment's average width (**d**). Propagation of thicker cellular segments was only visible at the highest temporal resolution of 1 image/5 s, which is why the majority of data points are concentrated at the bottom left corner of the graph. These measurements are plotted separately **e** for better visualization. The velocity of propagation of BAX recruitment significantly correlated with process thickness (rank Spearman correlation, $rs[36] = 0.784$, $p < 0.001$), with thicker segments exhibiting higher velocities

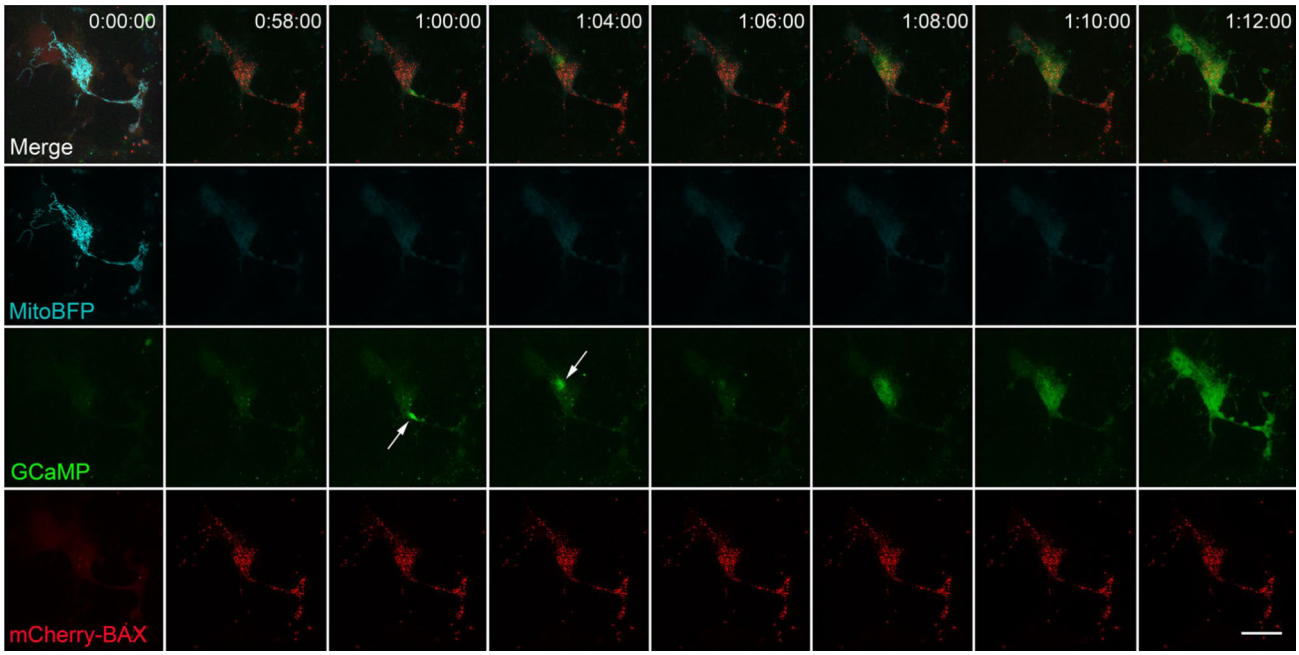

Fig. 6.

Calcium bursts and a final calcium wave occur after BAX propagation. The cell shown was nucleofected with mCherry-BAX, Mito-BFP, and pN1-GCaMP6m-XC (GCamP). The frame just before BAX recruitment initiation (approximately 24 h after STS addition) is shown in the left-most column. BAX recruitment propagated from the bottom right process to the soma (Supplemental Video 4) and was complete in 58 min. Discrete calcium spikes were then observed 60 and 64 min post BAX recruitment initiation (arrows). A final calcium wave was then recorded between 68–72 min post BAX initiation. The pattern of a final calcium wave was consistent for all propagating cells imaged with GCamP. The discrete bursts of calcium release that preceded the final wave were only apparent in cells imaged at a temporal resolution of 1 image every 2 min or less. Size bar = 10 μm

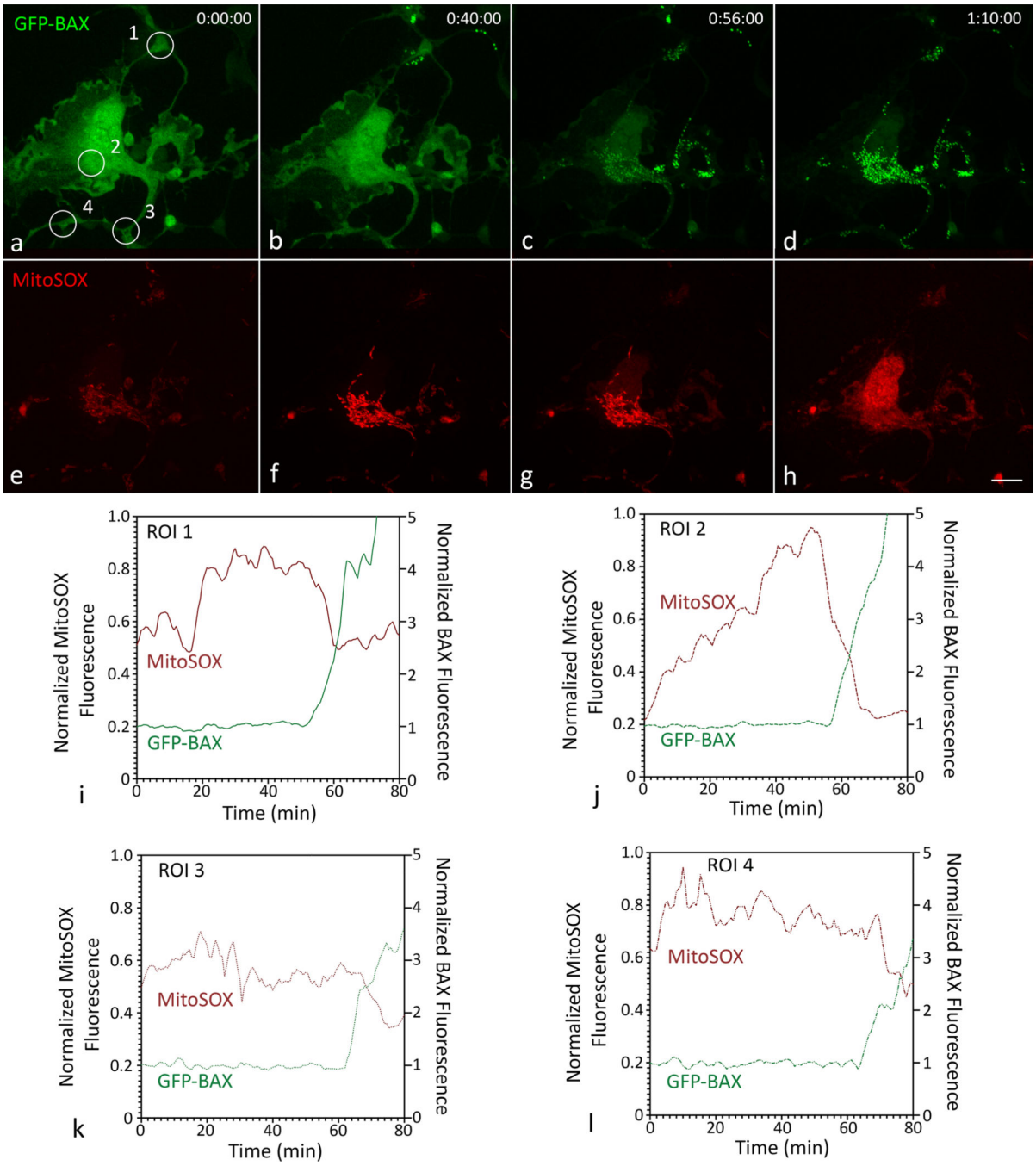

Fig. 7.

MitoSOX fluorescence in a propagating ARPE-19 cell. The cell shown was nucleofected with GFP-BAX and Mito-BFP (not shown), grown for 24 h, and incubated with MitoSOX at a final concentration of 4 μM for 8 min. Death was induced with 1 μM STS. **a** Diffuse BAX with regions of interest (ROI) shown as numbered circles. BAX recruitment initiated in the top left of the image (**b**) and propagated through the soma **c** to the bottom process **d** (see also Supplemental Video 5). MitoSOX fluorescence was initially dim and localized to the mitochondria (**e**). In the cell, particularly in the soma, mitochondrial MitoSOX fluorescence

increased prior to BAX recruitment (**f–g**), a phenomenon that was consistently observed in all 12 cells imaged. During BAX recruitment, mitochondrial MitoSOX fluorescence decreased and became diffuse (**h**). Size bar = 10 μm. The fluorescent intensities of GFP-BAX and MitoSOX at ROIs 1–4 were exported, normalized (GFP-BAX to baseline, MitoSOX to its maximum intensity), and plotted (**i–l**). An overlay of all these graphs is plotted in Supplemental Fig. S1 to better visualize the propagation of BAX initiation. In each ROI, the fluorescent intensity of mitochondrial MitoSOX rapidly decreased during the recruitment of GFP-BAX, possibly as a result of MOMP

Table 1

Summary of findings documenting the propagation of apoptotic events

Model and Stimulus	What propagates? (velocity)	What affects propagation?	What doesn't affect propagation	Reference
Mouse olfactory receptor neurons (in vivo). Induction by bulbectomy	Caspase-3 and caspase-9 activation (N/A: not live cell imaged)	Nothing Reported	Nothing Reported	Cowan et al. 2001 [1]
Permeabilized H9c2 cells. Induction by C2 ceramide or ethanol	Calcium waves (20 μm/sec fast wave followed by larger 40 μm/min slow wave). Slow wave coupled with mitochondrial depolarization	Calcium chelation (EGTA) and RuRed arrested calcium waves and depolarization. Increased calcium accelerated waves $BCLX_L$ expression reduced waves in some cells	Pan-caspase inhibition[a] or Thapsigargin + Ryanodine had no effect	Pacher and Hajnóczky 2001 [2]
HeLa cells fused to mouse embryonic fibroblasts. Induction by STS, FasL, or BH3I	CCR (~18 μm/min)	Nothing Reported	Mitochondrial depolarization did not propgate BAX and BAK ablation, calcium buffering and depletion of reticular calcium stores, and pan caspase inhibition[a] did not prevent CCR	Lartigue et al. 2008 [3]
Clustered HeLa cells. Induction by STS, TRAIL, or etoposide	CCR, SMAC/Diablo release, mitochondrial depolarization. (No velocities reported)	Thapsigargin with EGTA blocked CCR wave	BAPTA-AM or BAPTA-AM with EGTA had no effect	Bhola et al. 2009 [4]
Sibling HeLa cell pairs. Induction withSTS or TRAIL	CCR STS (10.2–18 μm/min) TRAIL (34–37 μm/min)	Inhibition of BID phosphorylase CK2 reduces TRAIL-induced wave	Nothing Reported	Rehm et al. 2009 [5]
Intact H9c2 cells. Induction with TNFα Permeabilized H9c2 cells or permeabilized HCM cells. Induction with tBID	CCR Intact H9c2 cells (13.8 μm/ min) Permeabilized H9cs cells (11.4 μm/ min) Permeabilized HCM cells (18.6 μm/ min)	MnTMPyP and SOD2 reduced propagation velocities	Pan caspase inhibition[a], EGTA, RuRed, and CsA had no effect	Garcia-Perez et al. 2012 [6]
Primary cultures of human syncytiotrophoblasts Spontaneous induction, or induction with $CoCl_2$ or Rotenone	Mitochondrial depolarization and nuclear chromatin condensation (~4.5 μm/min)	Nothing Reported	Nothing Reported	Longtine et al. 2012 [7]
Xenopus laevis egg cytosol extracts Induced with cytochrome c	Mitochondrial depolarization and caspase activation (~30 μm/min)	BCL2 addition, caspase 3 inhibition[a], and decreased mitochondrial concentration slowed propagation velocity	Nothing Reported	Cheng and Ferrell 2018 [8]

BAMPTA-AM, cell permeant calcium chelator; BAX and BAK, full length pro-apoptotic effector proteins of the BCL2 gene family; $BCLX_L$, anti-apoptotic member of the BCL2 gene family; BH3I, tBID mimetic; BID and tBID, BH3-only member of the BCL2 gene family-BID is processed to tBID by caspase activation in the extrinsic apoptotic pathway; *CCR* cytochrome c release; *CsA* cyclosporine A-permeability transition pore inhibitor; *EGTA* ethylene glycol-bis(β-aminoethyl ether)-N,N,N',N',-tetraacetic acid-calcium chelator; *FasL* Fas Ligand-transmembrane protein that binds to a death receptor to induce extrinsic apoptosis; *MnTMPyP* a celi permeant SOD mimetic that reduces oxidative stress; Rotenone, inhibits the electron transport chain (complex I); *RuRed* Ruthenium red-inhibits calcium release from intracellular stores and blocks uptake and release of calcium from mitochondria; Ryanodine, binds to and inhibits ryanodine calcium channels-blocks calcium release from endoplasmic reticulum; SMAC/Diablo, small mitochondrial protein released by mitochondrial outer membrane permeabilization- "second mitochondria-derived activator of caspase"; *SOD2* Superoxide dismutase 2-reduces oxidative stress; *STS* staurosporine; Thapsigargin, inhibitor of sarco-endoplasmic reticulum Ca2 + ATPase (SERCA)-promotes release of intracellular calcium stores; *TNFα* Tumor Necrosis Factor alpha; *TRAIL* TNF-related apoptosis-inducing ligand-stimulate extrinsic apoptotic pathway

[a]Caspase 3 Inhibition was achieved using Ac-DEVD-CHO. Pan caspase Inhibition was achieved using zVAD-FMK